ACS APPLIED MATERIALS & INTERFACES

RESEARCH ARTICLE

www.acsami.org

Surface-Enhanced Raman Detection of Melamine on Silver-Nanoparticle-Decorated Silver/Carbon Nanospheres: Effect of Metal Ions

Li-Miao Chen* and You-Nian Liu

College of Chemistry and Chemical Engineering, Central South University, Changsha 410083, PR China

ABSTRACT: Silver/carbon (Ag/C) core−shell nanospheres synthesized by a hydrothermal method were used as templates for fabricating silver nanoparticle-decorated Ag/C (Ag/C/AgNps) nanospheres. The particle size of Ag nanoparticles can be tuned by varying the concentration of Ag precursor. Detection of melamine molecules at concentrations as low as 5.0×10^{-8} M shows that the Ag/C/AgNps nanosphere is a good SERS-active substrate. The effect of heavy metal ions on the detection of melamine is also investigated. It was found that the SERS spectrum profile of melamine is very sensitive to the presence of heavy metal ions: the peak positions of the SERS bands exhibit some apparent change with the kind of metal ion, showing a blue or red shift compared with those in the SERS spectrum of melamine; the SERS signal intensity decrease with increasing the concentration of metal ion.

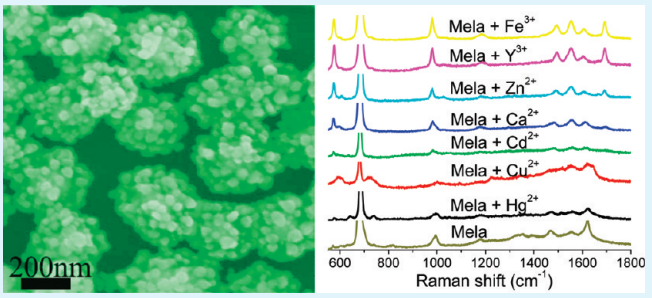

KEYWORDS: silver nanoparticle, surface-enhanced Raman scattering, carbon nanosphere, nanoparticle assembly, melamine, heavy metal ion

1. INTRODUCTION

Surface-enhanced Raman scattering (SERS) has recently been demonstrated to have potential for application in various fields, including analytical chemistry, life science, medical science, and the characterization of trace chemical species,[1−5] but for the most part the technique remains limited to laboratory use. One of the major difficulties in developing commercial applications of SERS has been the technological challenge of fabricating the substrates. To move SERS into the field, the problem of sensitivity, reproducibility, stability, substrate cost, and ease of manufacturing need to be addressed. Up to now, various approaches have been developed to fabricate SERS substrates with high sensitivity. Structurally, most SERS substrates are made from pure metallic nanostructures, in particular Ag and Au with various morphologies, such as nanoparticles, nanocubes, nanorods, nanosheets, nanowires, nanospheres, core−shell nanoparticles, and thin films.[6−11] Recently, a type of hybrid nanostructure, which combines a dielectric core with a layer of noble metals nanoparticles was used as SERS substrate and exhibited promising potentials.[12−17] These hybrid nanostructures have advantages over the conventional pure bimetallic noble metal nanostructures, such as higher SERS activity and lower cost when used as SERS substrates. Several kinds of nanomaterials including ZnO nanoarrays or nanospheres,[12−14] carbon nanotubes (CNTs),[15,16] SiO_2 nanofibers or nanospheres,[17−19] Si nanowires,[20,21] Ga_2O_3 nanowires,[22] TiO_2 nanoarrays,[23] and polymer spheres[24] have been used as templates to fabricate such hybrid nanostructure. As a semiconductor material, ZnO is practically cheap, nontoxic, and biosafe materials, and thus of special interest for biomolecular detection.[25] Moreover, it is easy to deposit Ag or Au nanoparticles on the surface of ZnO nanorods or nanospheres. However, ZnO nanomaterials may suffer from serious corrosion in solution due to their weak resistance to acids, bases and solvents. Compared with other materials, CNTs are more stable and can be easily synthesized with large scale. However, it has not been routine to fabricate even CNTs/Ag core−shell nanostructures. The most widely used methods for preparation of C/Ag including electrochemical and other chemical or physical approaches, either require pretreatment of pristine CNTs, such as oxidation by strong oxidizing acid or functionalization with a surfactant or polyelectrolyte.[26,27] The acid treatment of CNTs concerning their functional characteristics can damage and shorten CNTs due to bond fissure. CNTs/Ag core−shell nanostructures synthesized by these methods usually retain impurities such as surfactant or polyelectrolyte. which will influence ultrasensitive detection. Moreover, these methods clearly suffer through manipulation of complex experimental parameters and/or time-consuming steps for immobilization. Therefore, how to develop facile and feasible methods to prepare hybrid nanostructure based on noble metal nanoparticles and nanorods, wires, tubes, or spheres with high chemical stability still remains a challenge to materials scientists.

Recently, in China, adulteration by a high melamine level has been discovered in milk products.[28] The combination of melamine at high doses may lead to the formation of insoluble crystals in the kidneys, causing renal failure in humans.[29] Consequently, monitoring the level of melamine in milk products becomes very urgent for public health and food safety. Up to now, several methods including a low-temperature plasma probe combined

Received: May 15, 2011
Accepted: July 11, 2011
Published: July 11, 2011

with tandem mass spectrometry,[30] liquid chromatography/tandem mass spectrometry,[31] and mass spectrometry[32] have been developed for the detection of melamine in complex mixtures such as porcine muscle tissue and food. However, these methods require time-consuming and cumbersome sample pretreatment such as extraction, preconcentration, and derivatization. On the other hand, the "fingerprint-like" Raman spectrum is capable of providing overall and specific information on various chemical and biochemical components in a complex system without destroying the sample and requires little or no sample preparation.[33] However, up to now, there have been few reports on detecting melamine or detecting melamine from the milk products by SERS technique.[34−36] Usually, in the commercial milk products, there are many kinds of metal ions such as Zn^{2+}, Ca^{2+}, Fe^{3+}, etc., which is necessary to people's health. These metal ions may interact with melamine to form relative stable complexes. Therefore, investigation of the influence of metal ions in the SERS detection melamine is also very interesting.

In this work, Ag/C core−shell nanospheres synthesized by a hydrothermal method were used as templates for fabricating Ag/C/AgNps hybrid nanostructures. As-prepared Ag/C core−shell nanospheres possess large number of functional groups such as OH and CHO,[37] which can improve the hydrophilicity and stability of these nanospheres in aqueous system and react with metal ions to form metal nanparticles. Therefore, Ag/C/AgNps nanospheres could be fabricated using a solution method without using any linking molecules. The size of Ag nanoparticles deposited on Ag/C nanospheres can be adjusted simply by varying the concentration of Ag precursor. The resulting Ag/C/AgNps nanostructures can server as a good SERS substrates, exhibit a strong SERS enhancement effect, which enables the detection of melamine at a low concentration of 5.0×10^{-8} M. Finally, the effect of heavy metal ions on the detection of melamine is also investigated. It was found that the SERS spectrum profile of melamine is very sensitive to the presence of heavy metal ions.

2. EXPERIMENTAL SECTION

2.1. Synthesis of Ag/C Core−Shell and Carbon Nanospheres. Monodisperse Ag/C nanospheres were prepared by a modified hydrothermal synthesis as described in detail elsewhere.[37] Typically, 0.5 g of sugar and 0.01g $AgNO_3$ were dissolved in 30 mL of water to form a clear solution. After being stirred for more 30 min, the solution was then transferred to a stainless steel autoclave (50 ml in volume) and heated at 180 °C for 3 h after sealing. After the reaction, the autoclave was allowed to cool in air naturally. The suspension was then taken out and centrifuged at 8000 rpm for 10 minutes. The product was washed with de-ionized water and re-dispersed in de-ionized water. The centrifugation/rinsing cycles were then repeated three more times to obtain pure Ag/C core-shell nanospheres. For comparison, carbon nanospheres were also prepared in the absence of $AgNO_3$. All the steps were the same as in the synthesis of the Ag/C core-shell nanospheres.

2.2. Synthesis of Ag-Nanoparticle-Decorated Ag/C and Carbon Nanospheres. Fifty milligrams of the as-prepared Ag/C core−shell nanospheres were dispersed in 15 mL of water with the aid of ultrasonication to obtain a suspension. Ten microliters of $AgNO_3$ solutions with different concentrations (0.5−2.5 mM) was added to the suspension drop by drop under magnetic stirring at room temperature. After the Ag^+ ions were adsorbed onto the surface of Ag/C nanospheres for around 1 h via electrostatic attraction between Ag^+ ions and the negatively charged Ag/C surface, the suspension was added to 15 mL of sodium citrate solution (0.5 mM) and stirred for another 30 min. Finally, the dispersion was transferred into a 50 mL stainless steel autoclave. Hydrothermal synthesis was carried out at 110 °C for 1 h in an electric oven without stirring. The final product was first washed with acetone to remove excess sodium citrate and then washed multiple times with de-ionized water, following the wash−-centrifuge−redisperse purification cycle to obtain pure Ag/C/AgNP nanospheres. Ag-nanoparticles-decorated carbon (C/AgNP) nanospheres were also synthesized according the same procedures as described above.

2.3. Characterization. Morphologies and structures of the samples were characterized with scanning electron microscopy (SEM, Philips XL 30 FEG), transmission electron microscopy (TEM, Philips CM20, operated at 200 kV), and X-ray diffraction (XRD, Philips X'Pert MRD with Cu KR radiation). Ultraviolet−visible (UV−vis) spectra were recorded on an Aglient 8453 UV-vis Diode Array spectrophotometer. Raman measurements were conducted with a Renishaw 2000 laser Raman microscope equipped with a 633 nm laser of 2 μm spot size in diameter for excitation. All the spectra were acquired for 10 s with the laser power measured at the sample being 2.5 mW.

3. RESULTS AND DISCUSSION

The detailed information about the formation mechanism of the carbon nanospheres has been reported in other reports.[37] The morphology and microstructure of the products were studied using SEM, TEM and selected area electron diffraction (SAED). Typical low- and high-magnification SEM images of the samples prepared from the aqueous solution of sugar/$AgNO_3$ mixtures are shown in Figure 1a and b, which shows that as-synthesized particles are core-shell structures. The small white spots in the center of the nanospheres represent the Ag nanoparticles because the materials with heavier atomic mass may reflect much more electrons. The size of the core-shell structures is in the range of 150−400 nm. It was also found that the shape of the core-shell structures is affected by the shape of the core. For example, perfect nanospheres were formed when the cores are single spherical Ag nanoparticles, while elliptical nanoparticles were obtained when the cores are composed of several Ag nanoparticles. Figure 1c shows typical TEM image of core−shell Ag/C naostructures. The thickness of the shell is about 70 nm. The chemical composition of the core-shell nanoparticles is determined using the energy dispersive X-ray (EDX) spectrum of TEM. As shown in Figure 1d, there are four kinds of peaks in the EDX spectrum taken from a single core-shell structure, which corresponds to carbon, oxygen, silver, and copper elements, respectively. Strong copper peaks originate from the copper TEM grid that supports the sample, silver peak should comes from silver nanoparticle core; oxygen and carbon peaks should come from the shell. The selected area electron diffraction (SAED) pattern (the inset in Figure 1d) recorded from the silver core of a single core-shell nanoparticle indicates the single-crystalline nature of the silver core. For comparison, carbon nanoparticles were also prepared. Typical SEM image of the sample prepared in the absence of $AgNO_3$ under the identical other conditions used for preparing Ag/C core−shell structures is shown in Figure 1e, which shows that as-synthesized particles are spherelike nanoparticles. TEM image observation reveals that most the nanopartciles tended to aggregate into chainlike or branchlike structures. This suggests that presence of $AgNO_3$ leads to formation of nearly monodisperse nanospheres in the present system.

The morphology, phase and purity of crystal structure of the Ag/C/AgNps nanosphres prepared at different concentrations of $AgNO_3$ were studied using SEM, TEM, and XRD. Figure 2a

and b show low and high-magnification SEM images of the sample prepared with 1 mM $AgNO_3$, respectively. The coarse surfaces of the obtained nanospheres indicate the successfully coating Ag nanoparticles on the Ag/C nanospheres. As can be seen from Figure 2b, Ag nanoparticles with sizes of 5-15 nm are highly dispersed on the surface of Ag/C nanospheres. When the concentration of $AgNO_3$ was increased to 2.5 mM, Ag nanoparticles with bigger size (20−50 nm) were deposited on the surfaces of the Ag/C nanospheres (Figure 2c and d). Similar results could be observed using carbon nanospheres as the cores (Figure 2e and f). This means that the particle size of Ag nanoparticles on the surface of Ag/C or carbon nanospheres could be easily tuned by altering the concentration of $AgNO_3$. Figure 2g and h further present the TEM images of Ag/C/AgNps nanospheres prepared at 1 and 2.5 mM $AgNO_3$, respectively. Apparently, a dense Ag nanoshell formed on the surface of the spheres and the size of Ag nanoparticles on the surface increased greatly with increasing the concentration of $AgNO_3$. Figure 2i shows a high-resolution TEM (HRTEM) image of a single Ag nanoparticle. An interlayer spacing of about 0.20 nm was observed, in good agreement with the *d* spacing of Ag (200) lattice planes. The inset in Figure 2i is an SAED pattern of a single Ag/C/AgNps nanosphere. It shows that the SAED patterns are not bright concentric rings, but the ring patterns with intense spots. These rings are attributable to (111), (200), (220), (311) and (331) Ag fcc crystal diffractions. This confirmed that the as-synthesized Ag nanopatticles are crystallized in a phase similar to bulk Ag.[38] Figure 3 shows the XRD pattern of as-prepared Ag/C/AgNps nanospheres. All the diffraction peaks can be indexed to the (111), (200), (220), and (311) planes of the face-centered cubic (fcc) silver. After comparison we can find the intensity of the peaks increased with increasing the concentration of $AgNO_3$. This may be due to the relatively good crystallinity of Ag nanoparticles.

The UV−vis absorption spectra of carbon, Ag/C, and Ag/C/AgNP spheres are shown in Figure 4. All the samples were dispersed in ethanol for the UV−vis scan measurement. The bare

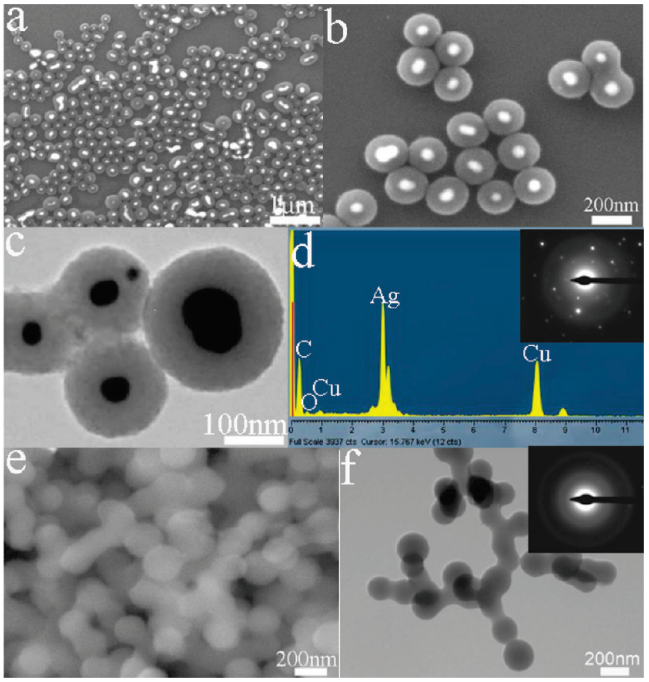

Figure 1. (a−c) SEM and SEM images of Ag/C core−shell nanospheres; (d) EDX spectrum of the Ag/C core-shell nanospheres, the inset is the corresponding SAED pattern; (e, f) SEM and TEM images of carbon nanospheres, the inset in f is the corresponding SAED pattern.

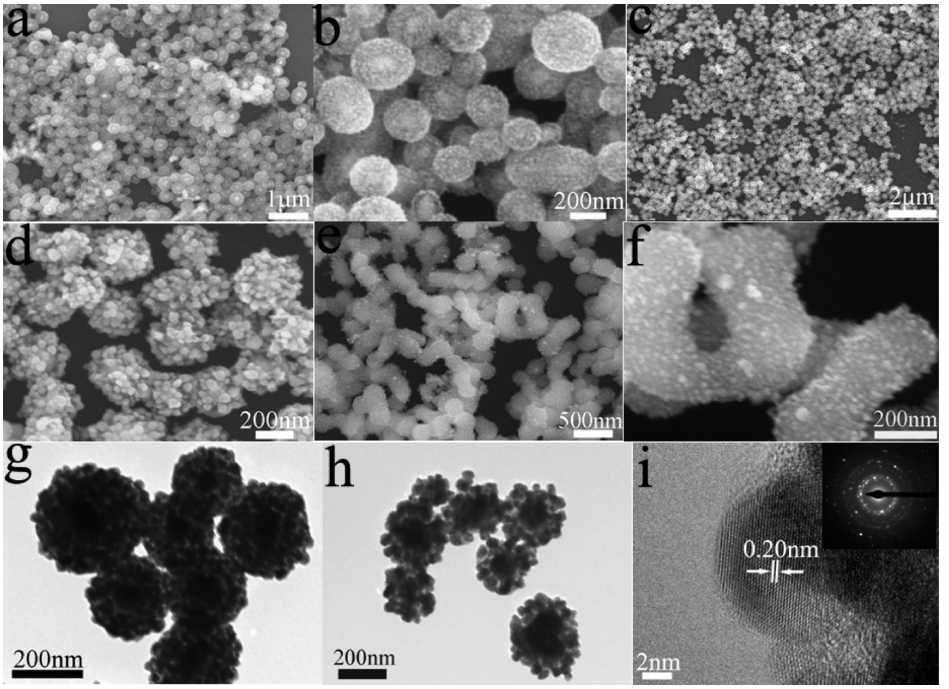

Figure 2. (a, b) SEM images of Ag/C/AgNps nanospheres prepared with 1 mM $AgNO_3$. (c, d) SEM images of Ag/C/AgNps nanospheres prepared with 2.5 mM $AgNO_3$. (e, f) SEM images of C/AgNps nanospheres prepared with 1 mM $AgNO_3$. (g, h) TEM images of Ag/C/AgNps nanospheres prepared with 1 and 2.5 mM $AgNO_3$, respectively. (i) Typical HRTEM image of an Ag nanoparticle on Ag/C/AgNps nanospheres, the inset is SAED pattern of a single Ag/C/AgNps nanosphere.

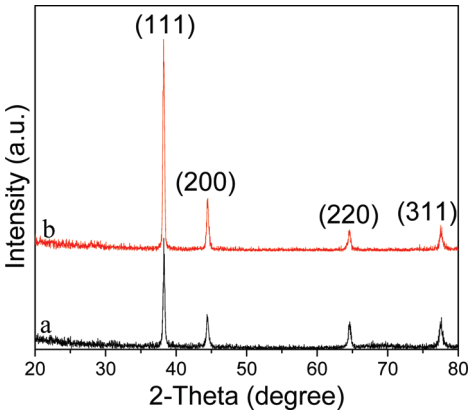

Figure 3. XRD patterns of Ag/C/AgNps nanospheres prepared with (a) 1 and (b) 2.5 mM $AgNO_3$.

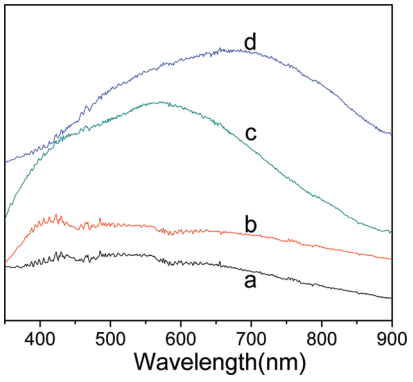

Figure 4. Absorption spectra of (a) carbon, (b) Ag/C, and Ag/C/AgNP spheres prepared with (c) 1 and (d) 2.5 mM $AgNO_3$.

carbon spheres have no distinct absorption peak (Figure 4a). For the Ag/C spheres, one weak peak appears at 420 nm (Figure 4b), which is attributed to the surface plasmon resonance (SPR) band of Ag cores.[39] Spectra c and d in Figure 4 show the Ag/C/AgNP spheres prepared at different concentration of $AgNO_3$. The composite spheres displayed an obvious broad and strong absorption in a wide range of 350−850 nm due to the Mie plasmon resonance excitation from the silver nanoparticles.[40] With increasing the size of the Ag nanopartcicles, the overall absorption increases, the SPR absorption peaks become broader and stronger, and their maxima red-shift from 550 to 680 nm. These changes may be attributed to the strong dipole−dipole coupling between neighboring Ag nanopartcicles and the inhomogeneity in size and shapes of Ag nanoparticles.[41−43]

The SERS enhancing properties of the Ag/C/AgNps nanospheres were studied using melamine as probe molecules. Figure 5 shows the SERS spectra of melamine solution deposited onto Ag/C/AgNps nanospheres; the spectra of melamine solution deposited on carbon and Ag/C nanospheres were also scanned for comparison. It was found that only one weak Raman peak assigned to melamine was identified at 1×10^{-4} M of melamine in the presence of carbon and Ag/C nanospheres, as shown in spectra a and b in Figure 5, but the Raman signals of melamine at the same concentration could be magnified significantly in the presence of Ag/C/AgNps composite spheres, as seen in Figure 5c and d. Detailed assignment of the spectra

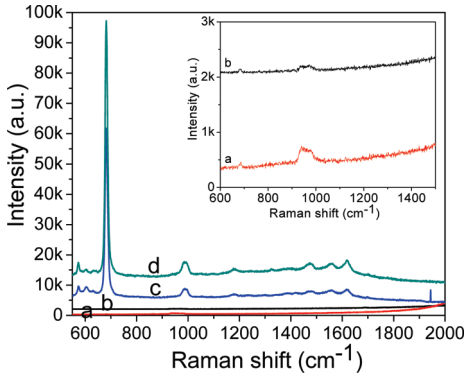

Figure 5. Typical SERS spectra of melamine (1×10^{-4} M) adsorbed on (a) carbon, (b) Ag/C nanospheres, and Ag/C/AgNP nanospheres prepared at different concentrations of $AgNO_3$: (c) 1 and (d) 2.5 mM. The inset is the SERS spectral region between 600 and 1500 cm^{-1}.

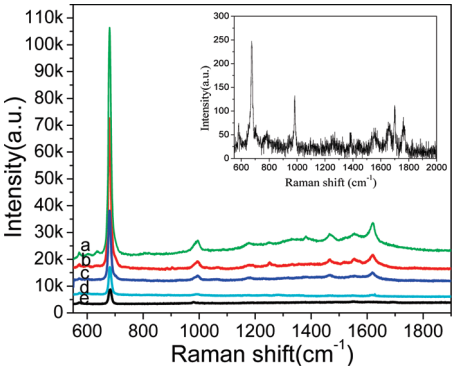

Figure 6. SERS spectra of melamine of various concentrations (a) 1.0×10^{-4} M, (b) 1.0×10^{-5} M, (c) 1.0×10^{-6} M, (d)1.0×10^{-7} M , (e) 5.0×10^{-8} M on Ag/C/AgNps nanospheres prepared at 2.5 mM $AgNO_3$. The inset is the SERS spectrum of bulk melamine.

features of melamine has been reported previously and will not be repeated here.[44,45] It was also found that the intensity of Raman signal at 682 cm^{-1} is higher on the Ag/C/AgNps nanospheres prepared with higher concentrations of $AgNO_3$. The increase in SERS intensity would be attributed to the increased size of Ag nanoparticles. Usually, SERS intensity could increase gradually with increasing the particle size and reaches a maximum at 110−130 nm.[46] Figure 6 shows the SERS spectra of melamine with various concentrations from1.0×10^{-4} to 5.0×10^{-8} M on Ag/C/AgNps nanospheres prepared with 2.5 mM $AgNO_3$. The Raman peak at 682 cm^{-1} remained clearly observable even if the concentration of melamine solution decreased to 5.0×10^{-8} M (Figure 6e). The SERS enhancement factor (EF) for melamine adsorbed on the Ag/C/AgNps nanospheres is calculated according to the equation[47] EF = $(I_{SERS}/I_{bulk})(N_{bulk}/N_{surface})$, where I_{SERS} and I_{bulk} denote the integrated intensities for the 682 cm^{-1} band of the 100 nM melamine adsorbed on Ag/C/AgNps nanospheres and bulk melamine on glass, respectively, whereas N_{SERS} and N_{bulk} represent the corresponding number of melamine molecules excited by the laser beam. For the target molecule melamine, in the sample area (1μm in diameter) measured, N_{SERS} was estimated to be about 3.0×10^5 molecules, assuming the melamine solution dispersed on the surface of Ag/C/AgNP nanospheres uniformly. Taking

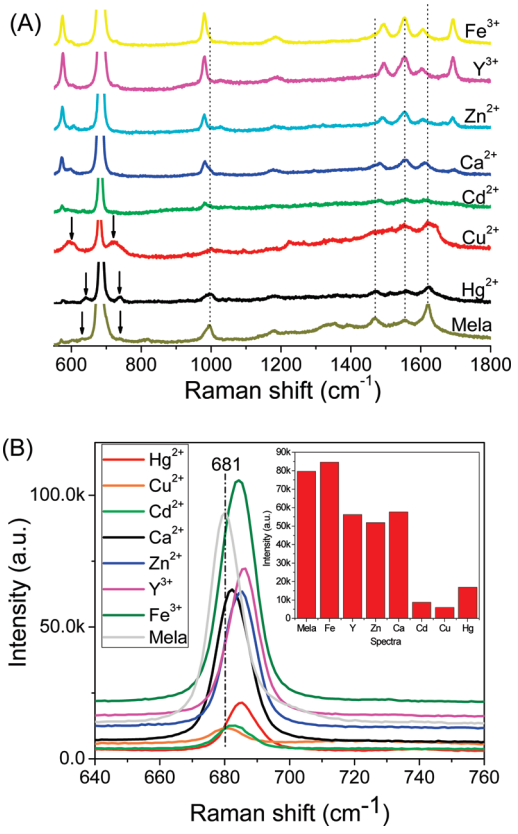

Figure 7. (A) SERS response of melamine (1.0×10^{-4} M) to various cations: Hg^{2+}, Cu^{2+}, Cd^{2+}, Ca^{2+}, Zn^{2+}, Y^{3+}, and Fe^{3+}. The concentration of metal ions in the melamine solution is 1.0×10^{-4} M. (B) SERS spectral region between 640 and 760 cm^{-1}. The inset is the dependence of the peak intensity of the band at about 682 cm^{-1} on the metal ions, in which the background of the signal has been removed in drawing the graph.

the laser spot (1 μm in diameter), the penetration depth (about 2 μm), and the density of melamine (1.57 g/mL) into account, N_{bulk} had a value of 1.2×10^{10} molecules in the detected solid sample area.[48] The EF of Ag/C/AgNP nanospheres is evaluated to be of the order of 1×10^7. These evidences indicated that the Ag/C/AgNP composite nanospheres as SERS substrates had good SERS performance.

Figure 7 shows the SERS spectra of melamine in the presence of various metal ions such as Hg^{2+}, Cu^{2+}, Cd^{2+}, Ca^{2+}, Zn^{2+}, Y^{3+}, and Fe^{3+}, whereas the spectrum of the melamine solution dispersed on Ag/C/AgNps nanospheres was also included for comparison. It was found that metal ions have great effects on the peak positions of the SERS bands, showing a blue or red shift compared with those in the SERS spectrum of pure melamine solution. In the presence of Cd^{2+}, Ca^{2+}, Zn^{2+}, Y^{3+}, and Fe^{3+}, the 998 and 1620 cm^{-1} bands show a red shift of 15−20 and 5−10 cm^{-1} to 978−982 and 1605−1611 cm^{-1} (Figure 7), respectively, while the 680 and 1468 cm^{-1} bands show a blue shift of 2−6 and 12−26 cm^{-1} to 682−686 and 1480−1494 cm^{-1}, respectively. Meanwhile, the SERS bands at 574, 1183, and 1552 cm^{-1} are unchangeable. Additionally, in the presence of Ca^{2+}, Zn^{2+}, Y^{3+}, and Fe^{3+}, a "new" peak was observed at 1696 cm^{-1}, which can be assigned to the ring distortion modes of melamine.[44,45] In the presence of Hg^{2+}, the 680 cm^{-1} band shows a blue shift of 5 cm^{-1} to 685 cm^{-1} and the bands at

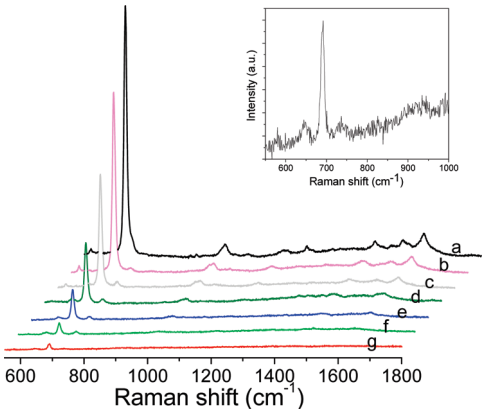

Figure 8. SERS spectra of melamine solution (1.0×10^{-6} M) with (a) 1.0×10^{-8} M, (b) 5.0×10^{-8} M, (c) 1.0×10^{-7} M, (d) 5.0×10^{-7} M, (e) 1.0×10^{-6} M, (f) 5.0×10^{-6} M, and (g) 1.0×10^{-5} M Hg^{2+}. The inset shows the special region of the SERS spectrum of melamine with 1×10^{-5} M Hg^{2+}.

640 and 740 cm^{-1} become apparent. In the presence of Cu^{2+}, the 740 cm^{-1} band shows a red shift of 15 cm^{-1} to 725 cm^{-1} and a broad band at 597 cm^{-1} was observed. It was also found that the Hg^{2+}, Cu^{2+}, and Cd^{2+} have a bigger influence in the SERS intensity of melamine than Ca^{2+}, Zn^{2+}, Y^{3+}, and Fe^{3+}. The aforementioned observations of spectral alteration suggest that the metal ions might interact with the melamine molecules (the NH group and/or N atom) to form a complex, leading to the reorganization of the adsorption model of melamine at the Ag surface and the related vibrations being weakened or enhanced.[49] The difference of the SERS spectrum profile of melamine in the presence of various metal ions may be due to the difference in the coordination surrounding between metal ions and melamine.

The effect of metal ion concentration on the SERS intensity of melamine was also investigated. A series of concentrations (1.0×10^{-5}, $5.0 \times 10^{-}$, 1.0×10^{-6}, 5.0×10^{-7}, 1.0×10^{-7}, 5.0×10^{-8}, and 1.0×10^{-8} M) of Hg^{2+} in melamine solution (1.0×10^{-6} M) were detected. Figure 8 shows the corresponding SERS spectra of the melamine solution with Hg^{2+} dispersed on Ag/C/AgNps nanospheres. It was found that the peak positions of 685 cm^{-1} band did not exhibit any change with the concentration of Hg^{2+}, while the intensity decreased greatly with increasing the concentration of Hg^{2+}. The peaks at 640 and 740 cm^{-1} were disappeared when the concentration of Hg^{2+} is lower than 5.0×10^{-8} M. These maybe indicate that the limit detection of Hg^{2+} for the melamine-Hg^{2+} system is about 5.0×10^{-8} M.

CONCLUSION

In summary, Ag/C/AgNps nanospheres were synthesized by a hydrothermal method in the $AgNO_3$ solution using sodium citrate as reducer. SEM, TEM, Raman spectroscopy. and UV−visible spectroscopy confirmed the formation of Ag/C/AgNp microstructures. The particle size of Ag nanoparticles was tuned by varying the concentration of Ag precursor. Raman analyses showed that the Ag/C/AgNps nanosphere is a good SERS-active substrate with melamine as test probe molecules. The enhancement factor for the Ag/C/AgNP nanospheres was on the order of 1×10^7. The effect of heavy metal ions on the detection of melamine is also investigated. It was found that the SERS spectrum profile of melamine is very sensitive to the presence of heavy metal ions. This aspect may allow one to qualitatively detect

heavy metal ions using the melamine−metal ion system. Moreover, on the basis of the contrasting SERS signal intensity, heavy metal ions such as Hg^{2+} and Cd^{2+} can be quasi-quantitatively detected.

AUTHOR INFORMATION

Corresponding Author
*E-mail: chenlimiao@csu.edu.cn.

ACKNOWLEDGMENT

This work was supported by the National Science Foundation of China (21076232).

REFERENCES

(1) Smith, W. E. *Chem. Soc. Rev.* **2008**, *37*, 955–964.
(2) Camden, J. P.; Dieringer, J. A.; Zhao, J.; Van Duyne, R. P. *Acc. Chem. Res.* **2008**, *41*, 1653–1661.
(3) Porter, M. D.; Lipert, R. J.; Siperko, L. M.; Wang, G.; Narayanan, R. *Chem. Soc. Rev.* **2008**, *37*, 1001–1011.
(4) Cao, Y. W. C.; Jin, R. C.; Mirkin, C. A. *Science* **2002**, *279*, 1536–1540.
(5) Graham, D.; Thompson, D. G.; Smith, W. E.; Faulds, K. *Nat. Nanotechnol.* **2008**, *3*, 548–551.
(6) Tao, A.; Kim, F.; Hess, C.; Goldberger, J.; He, R.; Sun, Y.; Xia, Y.; Yang, P. *Nano Lett* **2003**, *3*, 1229–1233.
(7) Shen, C.; Hui, C.; Yang, T.; Xiao, C.; Tian, J.; Bao, L.; Chen, S.; Ding, H.; Gao, H. *Chem. Mater.* **2008**, *20*, 6939–6944.
(8) Wang, H.; Kundu, J.; Halas, N. J. *Angew. Chem. Int. Ed.* **2007**, *46*, 9040–9046.
(9) Abdelsalam, M. E.; Mahajan, S.; Bartlett, P. N.; Baumberg, J. J.; Russell, A. E. *J. Am. Chem. Soc.* **2007**, *129*, 7399–7406.
(10) Nikoobakht, B.; El-Sayed, M. A. *J. Phys. Chem. A* **2003**, *107*, 3372–3378.
(11) Wang, T.; Hu, X.; Dong, S. *J. Phys. Chem. B* **2006**, *110*, 16930–16936.
(12) Song, W.; Wang, Y.; Hu, H.; Zhao, B. *J. Raman Spectrosc.* **2007**, *38*, 1320–1325.
(13) Zhao, X.; Zhang, B.; Ai, K.; Zhang, G.; Cao, L.; Liu, X.; Sun, H.; Wang, H.; Lu, L. *J. Mater. Chem.* **2009**, *19*, 5547–5553.
(14) Chen, L.; Luo, L.; Chen, Z.; Zhang, M.; Zapien, J. A.; Lee, C. S.; Lee, S. T. *J. Phys. Chem. C* **2010**, *114*, 93–100.
(15) Sun, Y.; Liu, K.; Miao, J.; Wang, Z.; Tian, B.; Zhang, L.; Li, Q.; Fan, S.; Jiang, K. *Nano Lett.* **2010**, *10*, 1747–1753.
(16) Chu, H.; Wang, J.; Ding, L.; Yuan, D.; Zhang, Y.; Liu, J.; Li, Y. *J. Am. Chem. Soc.* **2009**, *131*, 14310–14316.
(17) Kim, K.; Kim, H. S.; Park, H. K. *Langmuir* **2006**, *22*, 8083–8088.
(18) Zhang, S.; Ni, W.; Kou, X.; Yeung, M.; Sun, L.; Wang, J.; Yan, C. *Adv. Funct. Mater.* **2007**, *17*, 3258–3266.
(19) Sekhar, P. K.; Ramgir, N. S.; Bhansali, S. *J. Phys. Chem. C* **2008**, *112*, 1729–1734.
(20) Shao, M.; Zhang, M.; Wong, N.; Ma, D. D.; Wang, H.; Chen, W.; Lee, S. T. *Appl. Phys. Lett.* **2008**, *93*, 233118.
(21) Zhang, B.; Wang, H.; Lu, L.; Ai, K.; Zhang, G.; Cheng, X. *Adv. Funct. Mater.* **2008**, *18*, 2348–2355.
(22) Prokes, S. M.; Glembocki, O. J.; Rendell, R. W.; Ancona, M. G. *Appl. Phys. Lett.* **2007**, *90*, 093105.
(23) Li, X.; Chen, G.; Yang, L.; Jin, Z.; Liu, J. *Adv. Funct. Mater.* **2010**, *20*, 2815–2824.
(24) Yang, S.; Cai, W.; Kong, L.; Lei, Y. *Adv. Funct. Mater.* **2010**, *20*, 2527–2533.
(25) Shan, G.; Wang, S.; Fei, X.; Liu, Y.; Yang, G. *J. Phys. Chem. B* **2009**, *113*, 1468–1472.
(26) Raghuveer, M. S.; Agrawal, S.; Bishop, N.; Ramanath, G. *Chem. Mater.* **2006**, *18*, 1390–1393.
(27) Balasubramanian, K.; Sordan, R.; Burghard, M.; Kern, K. *Nano Lett.* **2004**, *4*, 827–830.
(28) Brown, C. A.; Jeong, K. S.; Poppenga, R. H.; Puschner, B.; Miller, D. M.; Ellis, A. E.; Kang, K. I.; Sum, S.; Cistola, A. M.; Brown, S. A. *J. Vet. Diagn. Invest.* **2007**, *19*, 525–531.
(29) Chan, E. Y. Y.; Griffiths, S. M.; Chan, C. W. *Lancet* **2008**, *372*, 1444–1445.
(30) Huang, G.; Ouyang, Z.; Cooks, R. G. *Chem. Commun.* **2009**, 556–558.
(31) Filigenzi, M. S.; Tor, E. R.; Poppenga, R. H.; Aston, L. A.; Puschner, B. *Rapid Commun. Mass Spectrom.* **2007**, *21*, 4027–4032.
(32) Vail, T. M.; Jones, P. R.; Sparkman, O. D. *J. Anal. Toxicol.* **2007**, *31*, 304–312.
(33) Yonzon, C. R.; Haynes, C. L.; Zhang, X. Y.; Walsh, J. T., Jr.; Van Duyne, R. P. *Anal. Chem.* **2004**, *76*, 78–85.
(34) Zhang, X. F.; Zou, M. Q.; Qi, X. H.; Liu, F.; Zhu, X. H.; Zhao, B. H. *J. Raman Spectrosc.* **2010**, *41*, 1365–1370.
(35) Zhang, B.; Xu, P.; Xie, X.; Wei, H.; Li, Z.; Mack, N. H.; Han, X.; Xu, H.; Wang, H. L. *J. Mater. Chem.* **2011**, *21*, 2495–2501.
(36) Lin, M.; He, L.; Awika, J.; Yang, L.; Ledoux, D.R.; Li, H.; Mustapha., A. *J. Food Sci.* **2008**, *73*, T129–T134.
(37) Sun, X.; Li, Y. *Langmuir* **2005**, *21*, 6019–6024.
(38) Chen, M.; Gao, L. *Inorg. Chem.* **2006**, *45*, 5145–5149.
(39) Sun, Y.; Yin, Y.; Mayers, B. T.; Herricks, T.; Xia, Y. *Chem. Mater.* **2002**, *14*, 4736–4745.
(40) Bohren, C. F.; Huffman, D. R. *Absorption and Scattering of Light by Small Particles*; John Wiley & Sons: Chichester, U.K., 1983.
(41) Wang, W.; Asher, S. A. *J. Am. Chem. Soc.* **2001**, *123*, 12528–12535.
(42) Peceros, K. E.; Xu, X. D.; Bulcock, S. R.; Cortie, M. B. *J. Phys. Chem. B* **2005**, *109*, 21516–21520.
(43) Zhu, M. W.; Qian, G. D.; Ding, G. J.; Wang, Z. Y.; Wang, M. Q. *Mater. Chem. Phys.* **2006**, *96*, 489–493.
(44) Koglin, E.; Kip, B. J.; Meier, R. J. *J. Phys. Chem.* **1996**, *100*, 5078–5089.
(45) Meier, R. J.; Maple, J. R.; Hwang, M. J.; Hagler, A. T. *J. Phys. Chem.* **1995**, *99*, 5445–5456.
(46) Hu, J.; Li, J.; Ren, B.; Wu, D.; Sun, S.; Tian, Z. *J. Phys. Chem. C* **2007**, *111*, 1105–1112.
(47) Chaney, S. B.; Shanmukh, S.; Zhao, Y. P.; Dluhy, R. A. *Appl. Phys. Lett.* **2005**, *87*, 31908.
(48) Yu, H.; Zhang, J.; Zhang, H.; Liu, Z. *Langmuir* **1999**, *15*, 16–19.
(49) Zamarion, V. M.; Timm, R. A.; Araki, K.; Toma, H. E. *Inorg. Chem.* **2008**, *47*, 2934–1936.